STM JOURNALS

Emerging Trends in
Chemical Engineering

ISSN: 2349-4786
Volume 12, Issue 2, 2025
May–August
DOI (Journal): 10.37591/ETCE

https://journals.stmjournals.com/etce

Research ETCE

Synthesis, Spectral Characterization, and Computational Studies of Hydrazine Derivative

M. Neela[1], B. Premalatha[1,2,*], P. Punitha[1,3]

Abstract

(E)-1-(2,3-dimethoxybenzylidene)hydrazine (2,3-DMBH) was synthesized by a condensation reaction. Fourier transform infrared (FT-IR), ^{1}H nuclear magnetic resonance (NMR), and ^{13}C NMR spectra were recorded for this compound. The synthesized compounds were evaluated as potential drug candidates through ADME (absorption, distribution, metabolism, and excretion) analysis and Lipinski's rule verification. Molecular docking studies against six proteins using AUTO DOCK software showed promising results. Among them, 2,3-DMBH exhibited strong binding affinities, particularly with 3ERT (–5.44 kcal/mol), followed by 5F90, 7E9B, and 3EWD. These findings suggest that 2,3-DMBH is a promising drug candidate. Furthermore, analysis of nonlinear optical (NLO) properties shows that the molecule has considerable NLO activity and it strongly indicates that the compound possesses electronic properties. Highest occupied molecular orbital–lowest unoccupied molecular orbital (HOMO-LUMO) analysis proved that the compound possesses chemical stability. Mulliken population analysis for the compound shows the presence of intermolecular hydrogen bonding. Molecular electrostatic potential (MEP) diagram of the compound shows the electrophile and nucleophile activity.

Graphical Abstract

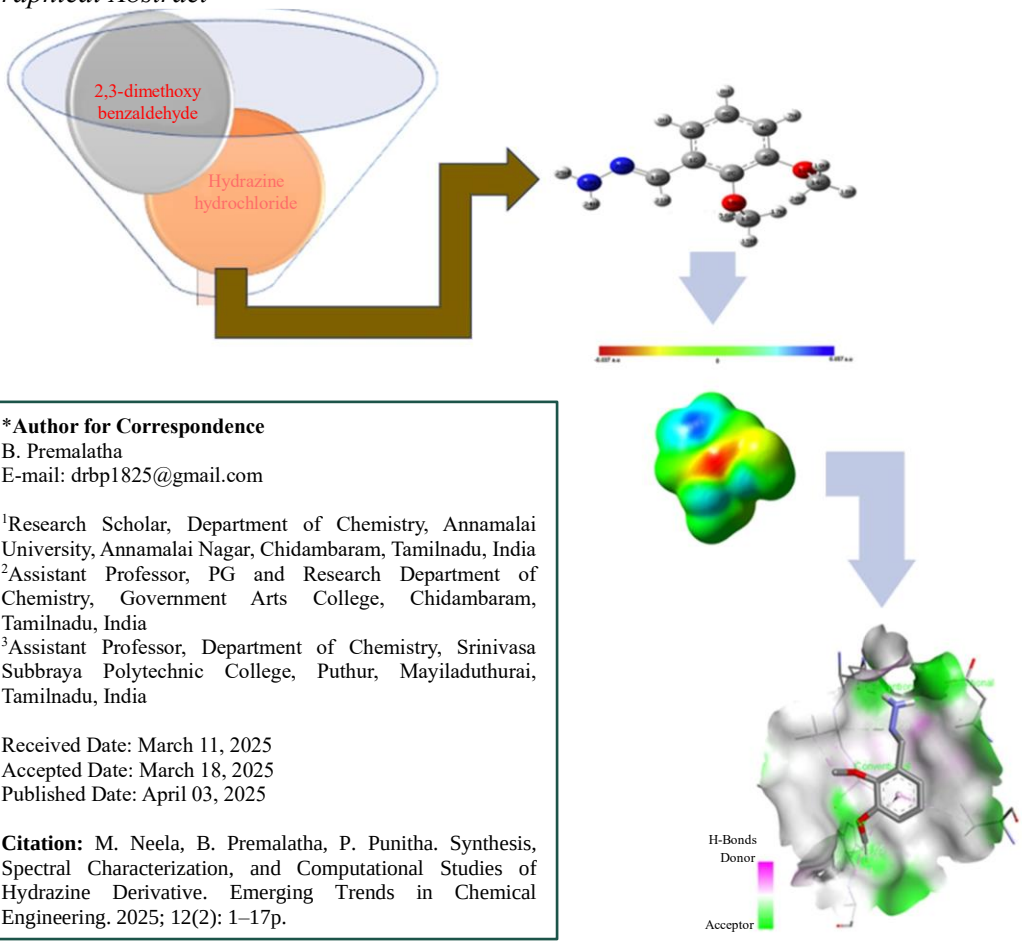

***Author for Correspondence**
B. Premalatha
E-mail: drbp1825@gmail.com

[1]Research Scholar, Department of Chemistry, Annamalai University, Annamalai Nagar, Chidambaram, Tamilnadu, India
[2]Assistant Professor, PG and Research Department of Chemistry, Government Arts College, Chidambaram, Tamilnadu, India
[3]Assistant Professor, Department of Chemistry, Srinivasa Subbraya Polytechnic College, Puthur, Mayiladuthurai, Tamilnadu, India

Received Date: March 11, 2025
Accepted Date: March 18, 2025
Published Date: April 03, 2025

Citation: M. Neela, B. Premalatha, P. Punitha. Synthesis, Spectral Characterization, and Computational Studies of Hydrazine Derivative. Emerging Trends in Chemical Engineering. 2025; 12(2): 1–17p.

Keywords: Nonlinear optical (NLO) activity, density functional theory (DFT) studies, highest occupied molecular orbital–lowest unoccupied molecular orbital (HOMO-LUMO), molecular electrostatic potential (MEP) diagram, Mulliken scale

INTRODUCTION

Schiff bases play a crucial role in medicine due to their diverse biological activities. They exhibit antimicrobial, anticancer, antioxidant, anti-inflammatory, and antiviral properties. Additionally, Schiff bases form metal complexes that enhance their therapeutic potential, including applications in neuroprotection, epilepsy treatment, and diabetes management. Their ability to interact with enzymes and cellular components makes them valuable for drug development and disease treatment [1–3]. 2,3-Dimethoxybenzaldehyde is an organic compound. It consists of a benzaldehyde core substituted with two methoxy (-OCH_3) groups at the second and third positions. This compound is widely used as an intermediate in organic synthesis, particularly in the production of pharmaceuticals, agrochemicals, and fragrances. The presence of methoxy groups enhances its reactivity, making it useful in Schiff base formation and other chemical transformations [4–7]. Additionally, it exhibits potential biological activities, including antimicrobial and antioxidant properties. Hydrazine hydrochloride plays a crucial role in organic synthesis, particularly in the preparation of Schiff bases, pharmaceuticals, and heterocyclic compounds. As a strong reducing and nucleophilic agent, it facilitates reactions such as hydrazone formation, cyclization, and condensation. In medicinal chemistry, it serves as a key intermediate in drug synthesis, contributing to the development of anticancer, antibacterial, and antifungal agents [8–10].

In Schiff bases, nonlinear optical (NLO) responses are typically influenced by various substituents, including electron-donating or electron-withdrawing groups [11]. These compounds are widely utilized due to their broad applications, ease of synthesis, and versatility in NLO research [12–15]. Computational methods play a crucial role in current scientific research by enabling accurate modeling, prediction, and optimization of materials and biological compounds. In the study of Schiff bases and NLO properties, computational techniques such as quantum mechanical calculations, particularly density functional theory (DFT), help predict molecular structures, electronic properties, and stability. These methods allow researchers to analyze polarizability, hyperpolarizability, and electronic transitions that influence NLO behavior [16–18]. Additionally, computational tools facilitate drug discovery by predicting Schiff base interactions with biological targets through molecular docking and dynamics simulations [19–22]. They also aid in exploring reaction mechanisms, optimizing synthetic routes, and designing advanced materials, including metal-Schiff base complexes for catalysis and electronics. By providing cost-effective, time-saving, and precise insights, computational studies significantly enhance experimental research and the development of novel compounds with improved properties [23–28].

Therefore, the proper synthesis and development of new Schiff bases are essential. Building on our previous studies, we have synthesized a Schiff base through the methanolic condensation of 2,3-dimethoxy benzaldehyde with hydrazine hydrochloride. Hydrazine derivatives have diverse biological applications, including anticancer, antimicrobial, antitubercular, antioxidant, and anti-inflammatory properties [29]. They are used in chemotherapy, tuberculosis treatment (isoniazid), and neurological disorders (monoamine oxidase [MAO] inhibitors). Additionally, they exhibit antiviral potential and enhance drug delivery through metal complexes, making them essential in pharmaceutical research and drug development. The evaluation of a Schiff base's NLO activity, resulting from substituting an aldehyde with a hydrazine derivative, may involve both computational simulations and experimental techniques. Computational studies are integral to NLO research, as they offer deep insights into the underlying mechanisms and facilitate the identification, design, and optimization of new materials with enhanced nonlinear optical properties. The NLO characteristics of the final product are influenced by the choice of aldehyde, which determines the overall molecular structure. This study focuses on the synthesis, characterization, and comparative analysis of Schiff bases derived from substituted hydrazine compounds, aiming to elucidate the structure-property relationships that govern their NLO and biological behavior.

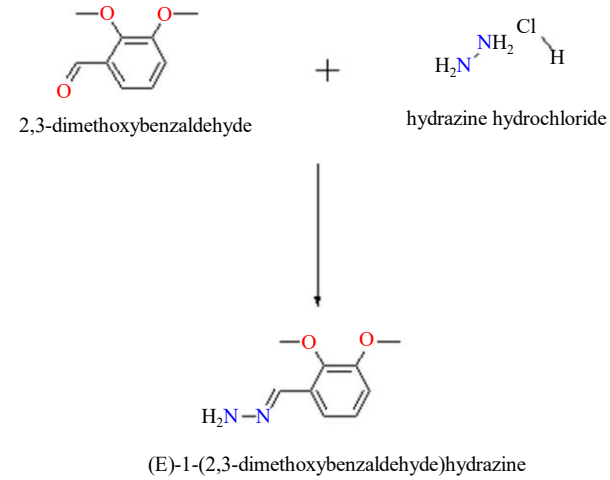

Scheme 1. Synthetic route of (E)-1-(2,3-dimethoxybenzylidene) hydrazine (2,3-DMBH).

MATERIALS AND METHODS

Synthetic Route

Approximately 0.498 g of 2,3-dimethoxybenaldehyde and 0.315 g of hydrazine hydrochloride were dissolved using methanol until the mixture becomes homogenous, and then few drops of acetic acid were added. The reaction mixture was stirred for up to 2 to 3 hours, after which the reaction mixture was filtered, and the filtrate was allowed to undergo slow evaporation process. After 2 days, orange colored crystals were obtained. The obtained product was characterized by spectroscopic techniques. Scheme 1 shows the synthetic route of (E)-1-(2,3-dimethoxybenzylidene) hydrazine.

Characterization Techniques

The synthesized product was characterized by spectroscopic techniques such as Fourier transform infrared (FT-IR) spectroscopy, nuclear magnetic resonance (NMR) analysis, ultraviolet (UV) spectra and theoretical studies like AUTO DOCK, absorption, distribution, metabolism, excretion, and toxicity (ADMET), and density functional theory (DFT) studies.

RESULTS AND DISCUSSION

FT-IR Spectrum

The FT-IR spectrum was captured in the 4000 to 400 cm^{-1} wavenumber range, as shown in Figure 1 and tabulated in Table 1. The presence of HC=N bond is confirmed by the band at 1621.50 cm^{-1}. The peak of the -NH stretching vibration is observed at 3384.40 cm^{-1}. The peak at 3087.66 cm^{-1} is attributed to the vibrations of aromatic C-H bonds. Stretching vibrations of C-O groups are found at 1266.21 cm^{-1}. The crystal structure of 2,3-DMBH correlates well with all of the detected FT-IR bands.

NMR Spectrum

^{1}H-NMR Spectral Data

Four signals are obtained for the protons with aromatic rings of both hydrazine hydrochloride and 2,3-dimethoxy benzaldehyde moiety in the region of 6.945 to 7.678 ppm. The singlet signal detected at 8.999 ppm was an azomethine proton (HC=N) bond between the hydrazine hydrochloride and 2,3-dimethoxy benzaldehyde. -NH proton that generates singlet signal at 2.104 ppm. The methoxy protons appeared at 3.835 and 3.848 ppm which correlates to six protons. Figure 2(a), and Table 2 show the ^{1}H-NMR spectrum of 2,3-DMBH.

^{13}C-NMR Spectral Data

There are six signals in ^{13}C-NMR that arise between 115.33 and 127.42 ppm and correspond to the aromatic carbons of both hydrazine hydrochloride and 2,3-dimethoxy benzaldehyde moieties. The signal at 54.84, 60.92 ppm is related with methoxy carbon (OCH_3). The signal at 157.08 ppm correlated

with carbon atom in azomethine (HC=N). Figure 2(b) and Table 3 show the 2,3-DMBH ^{13}C-NMR spectrum.

UV Absorbance Spectrum

UV–visible spectrophotometer is an essential equipment to provide the valuable factors about optical transparency, optical energy band gap and electronic band structures of the materials as well as the spectroscopic absorption of UV and visible light involves advancement of the electrons σ and π orbital from the ground state to the higher energy state [30–32]. The spectrum of optical transmittance for the 2,3-DMBH crystal with 2 mm thickness has been plotted within the range of 190 to 900 nm using a Perkin Elmer Lambda 35 UV–Vis spectrometer. The transmittance spectrum of the title material is active in the UV–visible region and acquires maximum transparency of about 66% in the visible and near IR regions with the lower cut-off wavelength being at 390 nm as shown in Figure 3. The optical energy band gap of the grown crystal is determined from the relation:

$$(\alpha h\upsilon)^2 = A(E_g - h\upsilon)$$

where E_g is the optical band gap of the given crystal and A is a constant. The band gap of the material was obtained by plotting the variation of $(\alpha h\upsilon)^2$versus $h\upsilon$ in the fundamental absorption region is shown in Figure 4. The energy band gap plot is drawn which is obtained by extrapolating the linear Tauc plot measure to the equivalent energy axis [33]. From this method, the value of optical energy band gap is found to be 4.69 eV. The high-energy band gap of the 2,3-DMBH crystal confirms the large transmittance in the visible region and defect concentration is less in the grown crystal [20]. The value of energy band gap and lower cut-off wavelength shows that the grown title material is suitable for the photonics and optical applications.

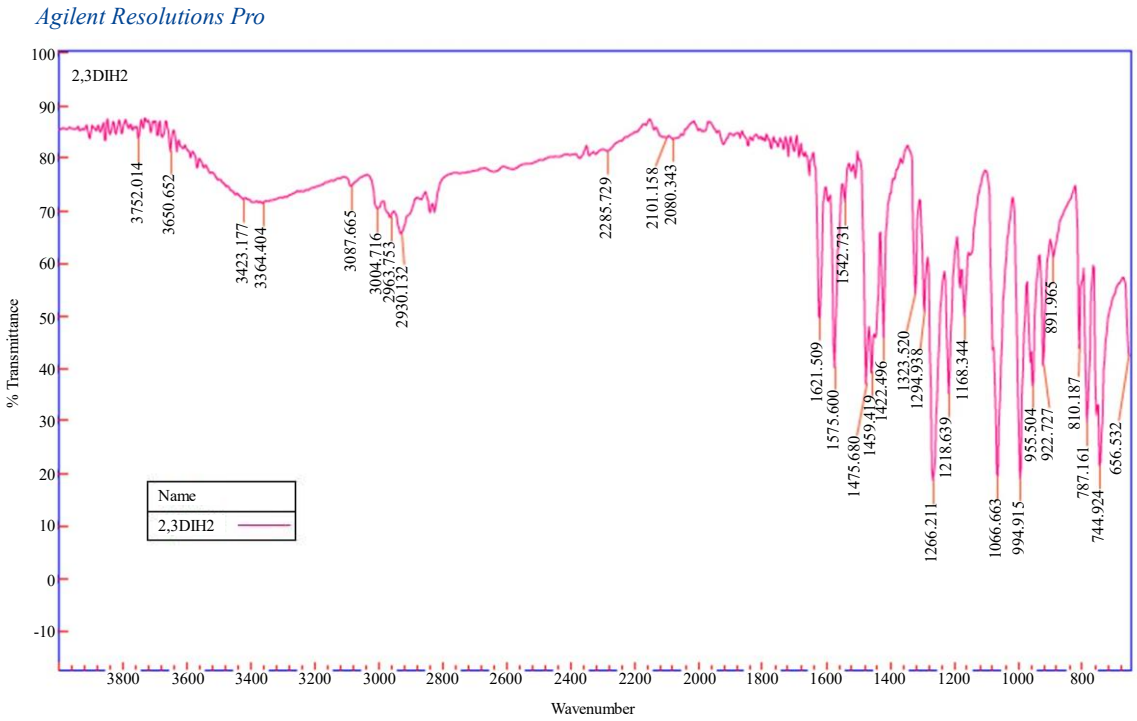

Figure 1. Fourier transform infrared (FT-IR) spectrum of (E)-1-(2,3-dimethoxybenzylidene) hydrazine (2,3-DMBH).

Table 1. Vibrational frequency assignment for (E)-1-(2,3-dimethoxybenzylidene) hydrazine (2,3-DMBH).

Functional Group	Aromatic	C=N	C-O	-NH$_2$
Frequency (cm^{-1})	3087.66	1621.5	1266.21	3354.40

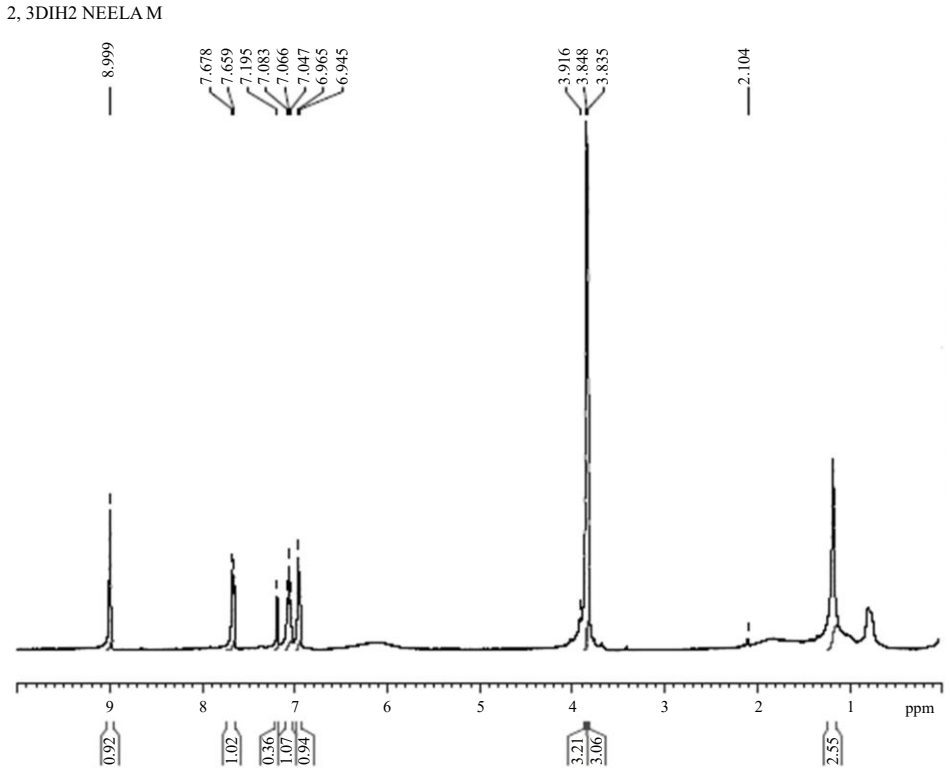

Figure 2. (a) ^{1}H-NMR spectrum of (E)-1-(2,3-dimethoxybenzylidene) hydrazine (2,3-DMBH).

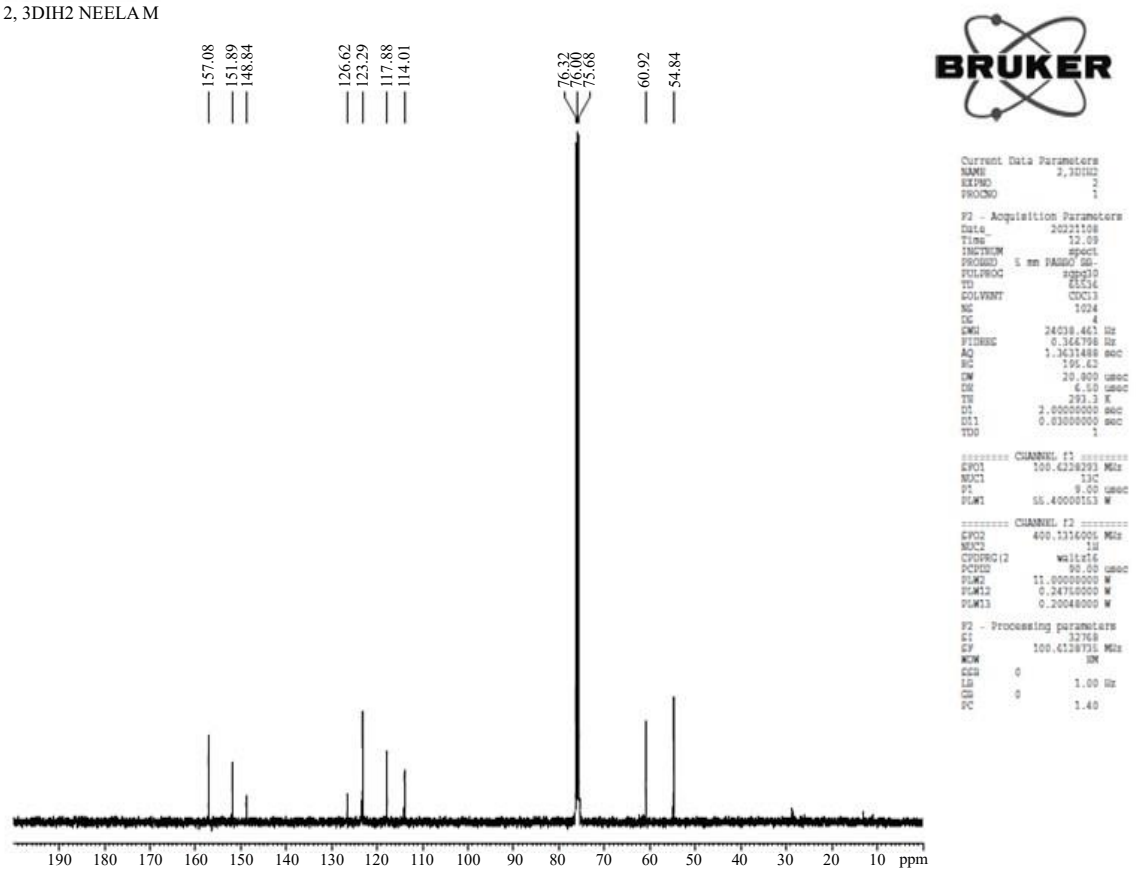

Figure 2. (b) ^{13}C-NMR spectrum of the (E)-1-(2,3-dimethoxybenzylidene) hydrazine (2,3-DMBH).

Table 2. ^{1}H-NMR table of (E)-1-(2,3-dimethoxybenzylidene) hydrazine (2,3-DMBH).

Functional Group	-NH_2	Aromatic proton	Azomethine (HC=N)	-OCH_3
Chemical shift (ppm)	2.104	6.945-7.678	8.999	3.835, 3.848

Table 3. ^{13}C-NMR spectrum table of (E)-1-(2,3-dimethoxybenzylidene) hydrazine (2,3-DMBH).

Functional Group	Aromatic carbon	Azomethine (HC=N)	OCH_3
Chemical shift (ppm)	115.33-127.42	157.08	54.84, 60.92

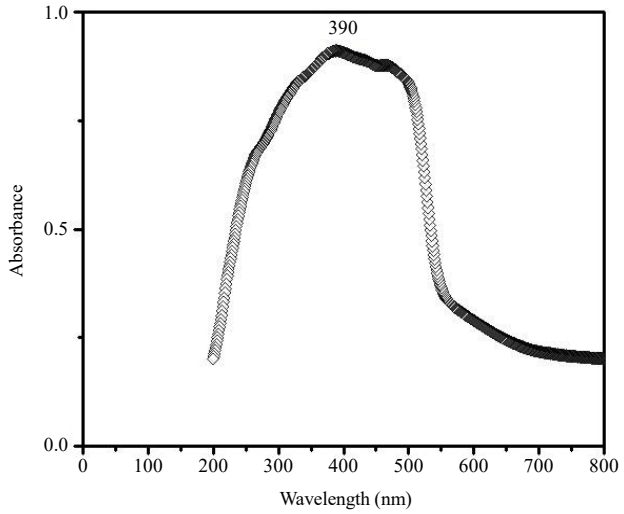

Figure 3. Ultraviolet (UV) absorbance spectrum of the (E)-1-(2,3-dimethoxybenzylidene) hydrazine (2,3-DMBH).

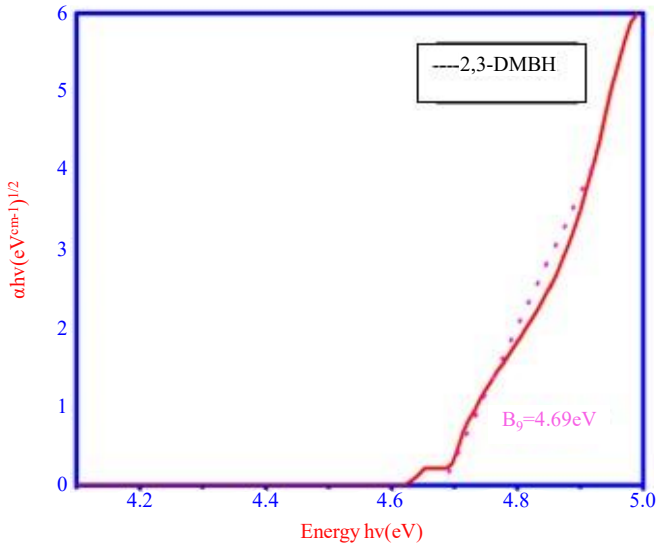

Figure 4. Tauc plot of (E)-1-(2,3-dimethoxybenzylidene) hydrazine (2,3-DMBH).

ADMET Properties

Drug development and research is a time-consuming and expensive procedure that comprises illness selection, identification of target and confirmation, lead generation and optimization, clinical trials, and preclinical trials [27]. Recently, in silico procedures for new entities at the molecular level have been authorised by the version. Prediction of in silico process is increasingly important in development of pharmaceutical research. Only 59 (64%) of the new medicines evaluated utilizing the ADMET characteristics were approved by the US Food and Drug Administration (FDA) in 2018. The Swiss

ADME program is quite useful for assessing the ADMET qualities and classifying the preliminary drug development process. The software mentioned here saves time, saves money, and decreases pollutants [28]. The synthesized compounds 2,3-DMBH was analyzed and compared with metformin and a detail report of the bioavailability of synthesized compound 2,3-DMBH is displayed in Table 3 and Figure 4.

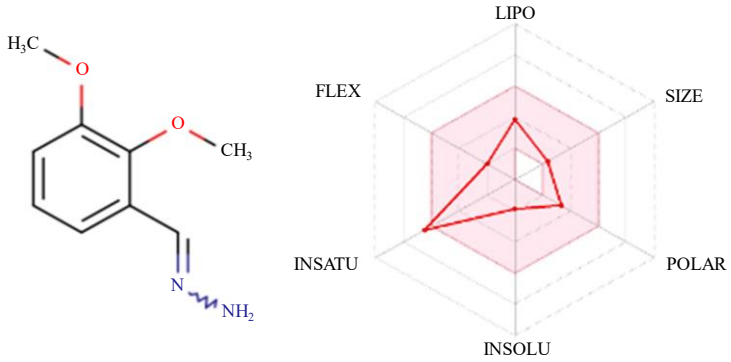

SMILES N/N=C\c1cccc(c1OC)OC

Figure 4. (E)-1-(2,3-dimethoxybenzylidene) hydrazine (2,3-DMBH) oral bio availability radar in ADME (absorption, distribution, metabolism, and excretion) prediction.

Table 4. Complete ADMET (absorption, distribution, metabolism, excretion, and toxicity) profile of (E)-1-(2,3-dimethoxybenzylidene) hydrazine (2,3-DMBH), including pharmacokinetics, physicochemical properties, lipophilicity, water solubility, drug-likeness, and medicinal chemistry.

Parameters	2,3-DMBH
Formula	$C_9H_{12}N_2O_2$
Molecular weight (g/mol)	180.20 g/mol
Num. of heavy atoms	13
Num. of aromatic heavy atoms	6
Num. of rotatable bonds	3
Num. H-bond acceptors	3
Num. H-bond donors	1
Molar refractivity	50.78
Topological polar surface area (TPSA) [Å]^2	56.84
Log $p_{o/w}$ [iLOGP]	1.71
Consensus Log $p_{o/w}$	1.24
Log s [*ESOL*]	-1.89
GI absorption	High
BBB permeant	Yes
P-gp substrate	No
CYP1A2 inhibitor	No
CYP2C19 inhibitor	No
CYP2C9 inhibitor	No
CYP2D6 inhibitor	No
CYP3A4 inhibitor	No
Log k_p [skin permeation cm/s]	-6.50
Lipinski	Yes, 0 Violation
Ghose	Yes
Veber	Yes
Muegge	No; 1 Violation: MW < 200
Bioavailability score	0.55
Lead-likeness	No; 1 Violation: MW < 250
Synthetic accessibility	1.93

ADME, which stands for absorption, distribution, metabolism, and excretion is an efficacy scale of any drug and Swiss ADME is a reliable online tool for estimating how chemically similar drug is to be a medicine and how it functions in the body [34, 35]. The ADME prediction of complex and ligands were researched to better understand, how changes in a structure affects the complex biological function. The six physicochemical variables, namely size, solubility, lipophilicity, flexibility, polarity, and saturation are being investigated by bioavailability radar (BR) makes the scientific studies within a short period of time [36], used to measure how similar incredible organic compounds is became as a medicine. Lipophilicity of a molecule is referred to as ligand permeation (log $P_{o/w}$), a feature that permits drugs to pass the cell's lipid bilayer membrane to reach the site of action and this determines its drug-like behavior and the octanol-water partition coefficient is widely used to calculate how much a ligand travels across a membrane. The fingerprint plots of compound 2,3-DMBH were used to explore the physicochemical properties of the drug candidates [37], and the full ADME properties are shown in Table 4 and Figure 4 and the pink region represents the ideal range for each compound characteristic.

Gastrointestinal Absorption and Brain Penetration Prediction [BOILED-Egg]

Some pharmaceutical ingredient developing attempts have been gastrointestinal absorption. The BOILED-Egg model provides a rapid, reproducible, straightforward, and statistically better method for calculating the high gastrointestinal absorption and high brain permeability of tiny compounds used in drug discovery and development [38]. Our compound 2,3-DMBH exhibit better pharmacokinetic and bioavailability characteristics, as seen in the approximated BOILED-Egg graphic (Figure 5).

Molecular Docking Studies

The selection and prioritization of target proteins for studies based on a disease and data mining methods by searching through literature and databases by which we obtained docking results with a greater number of proteins by searching through literature and database by which we obtained docking results with a greater number of proteins [39]. Our compound, have good binding affinity towards the proteins, which we have chosen from the PDB by its coded namely 3ERT, IQSG, 3EWD, 7E9B, 4NXI, and 5P90. The selected six types of target proteins were docked and found to have useful binding energy and the results obtained given in Table 5. The ligands frequently interact with the proteins via a variety of interactions, including as pi-alkyl interactions, pi-pi contacts, and pi-donor hydrogen bond interactions.

Molecular Docking Analysis of 3ERT (Anti-tumor Protein)

The human estrogen receptor alpha ligand binding domain was docked with the synthesized compound 2,3-DMBH 3ERT in complex with 4-hydroxytamoxifen. Compound 2,3-DMBH had a good binding energy (-4.43 kcal/mol) and a strong interaction with pi-pi stacked, pi-pi T-shaped, conventional hydrogen bonding at an angle of 2.88 Å, and pi-alkyl distance at a distance of 3.83 Å. Figure 6 shows the 2D and 3D image of compound 2,3-DMBH.

Molecular Docking Analysis of 3EWD (Anti-malarial Protein)

Crystal structure of adenosine deaminase mutant (delta Asp172) from plasmodium vivax in complex with MT-coformycin, 3EWD was docked with the compound 2,3-DMBH. In this compound 2,3-DMBH was found to provide a good binding energy (–4.43 kcal/mol) due to strong interactions with acceptor-acceptor, pi-sigma, conventional hydrogen bonding in the angle of 2.28 Å and pi-donor distance at 4.91 Å. The docking results of 2D and 3D images are given in Figure 7.

Table 5. Binding energy data of (E)-1-(2,3-dimethoxybenzylidene) hydrazine (2,3-DMBH) against different types of protein and the data will be compared with standard drugs.

Ligands	3ERT Binding Energy (kcal/mol)	3EWD Binding Energy (kcal/mol)	7E9B Binding Energy (kcal/mol)	5F90 Binding Energy (kcal/mol)
2,3-DMBH	-5.44	-4.43	-4.59	-4.71
Regorafenlb	-	-	-5.98	-
5-flurourocil	-	-	-	-2.99

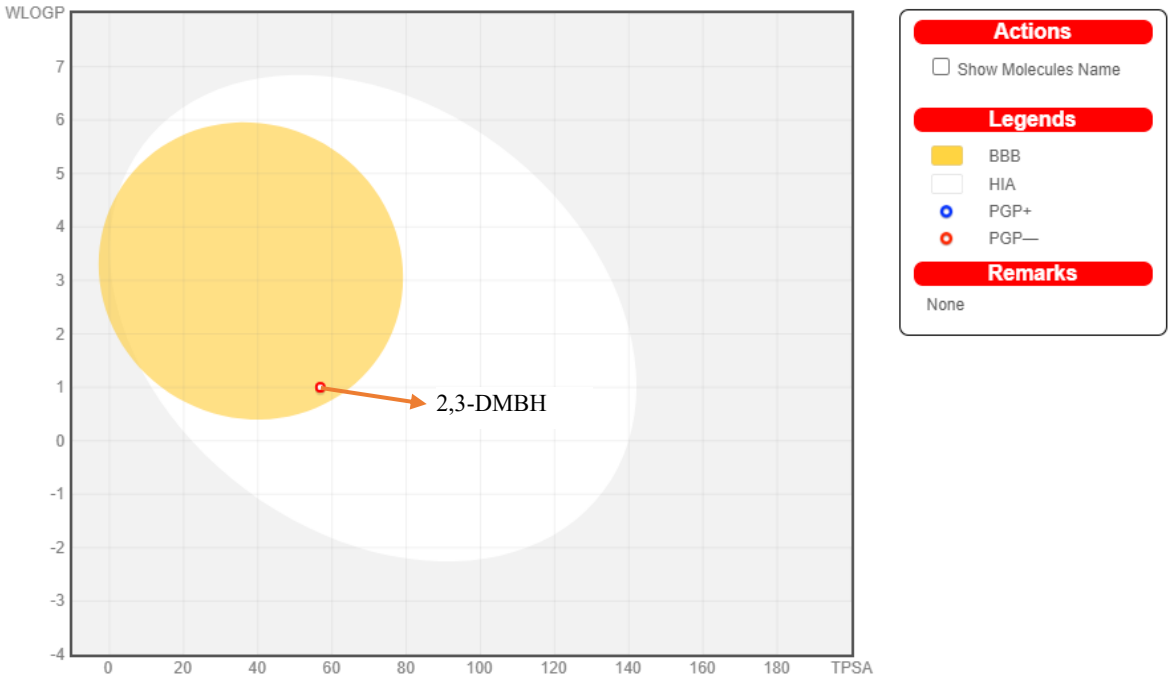

Figure 5. (E)-1-(2,3-dimethoxybenzylidene) hydrazine (2,3-DMBH) blood brain barrier (BBB) permeability (BOILED-Egg).

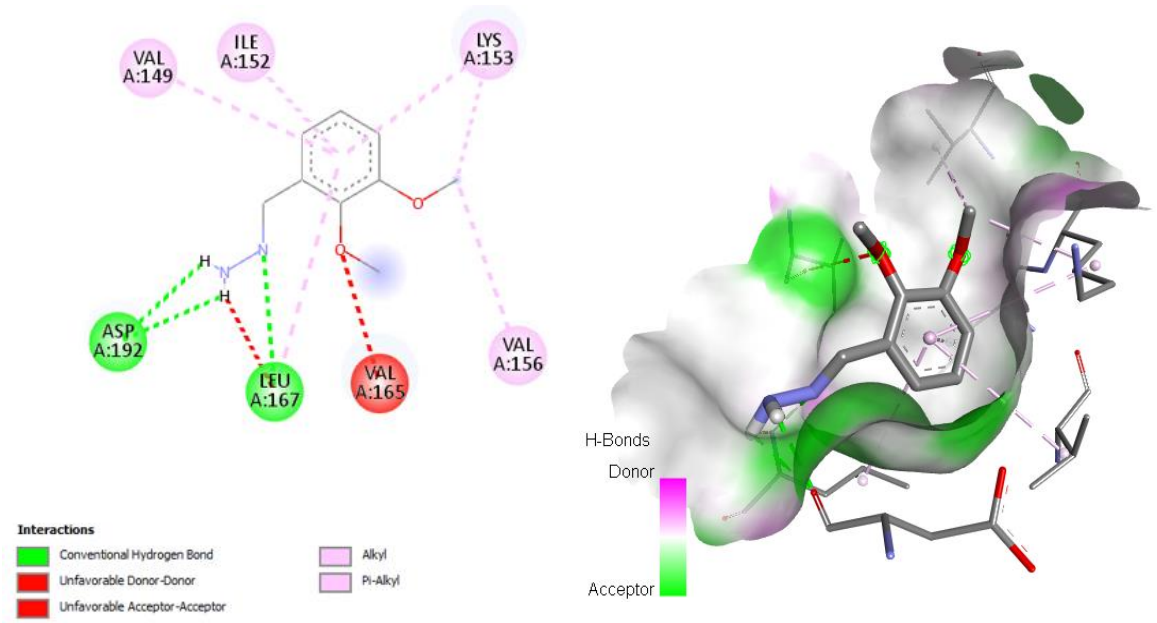

Figure 6. Docking images of compound (E)-1-(2,3-dimethoxybenzylidene) hydrazine (2,3-DMBH) against 3ERT.

Molecular Docking Analysis of 7E9B (Anti-cancer Protein)

Structural basis of HLX10 PD-1 receptor recognition, a promising anti-PD-1 antibody clinical candidate for cancer immunotherapy 7E9B was docked with synthesized derivative 2,3-DMBH.

In this compound, 2,3-DMBH was found with very good binding energy (-4.59 kcal/mol) owing to the strong interactions like acceptor-acceptor, pi-stacked, conventional hydrogen bonding in the angle of 2.50, 2.17 Å and pi-anion distance in 3.96 Å. The 2D and 3D images are given in Figure 8.

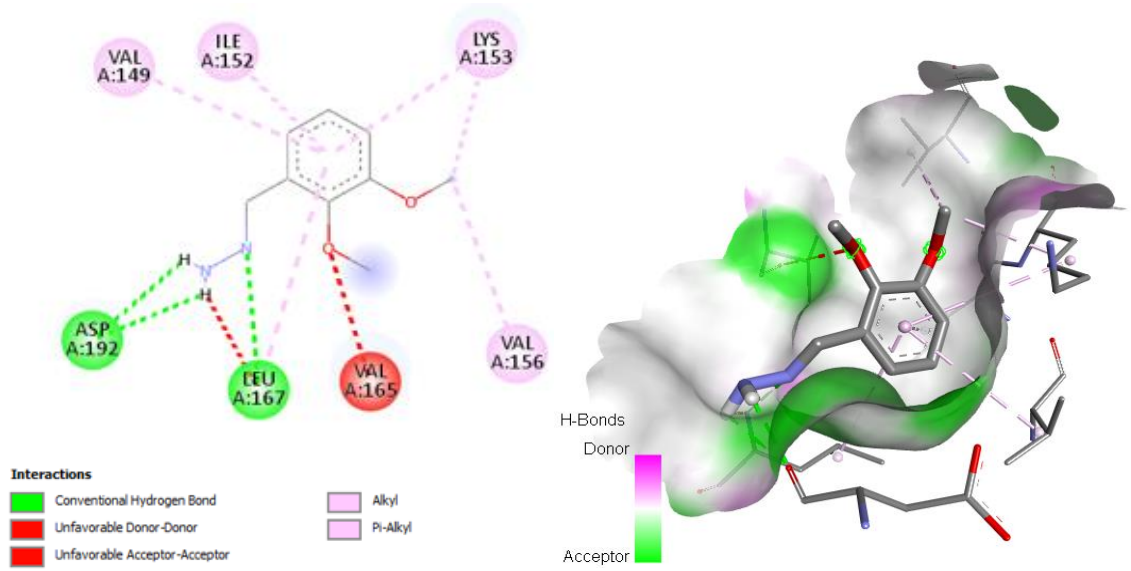

Figure 7. Docking images of compound (E)-1-(2,3-dimethoxybenzylidene) hydrazine (2,3-DMBH) against 3EWD.

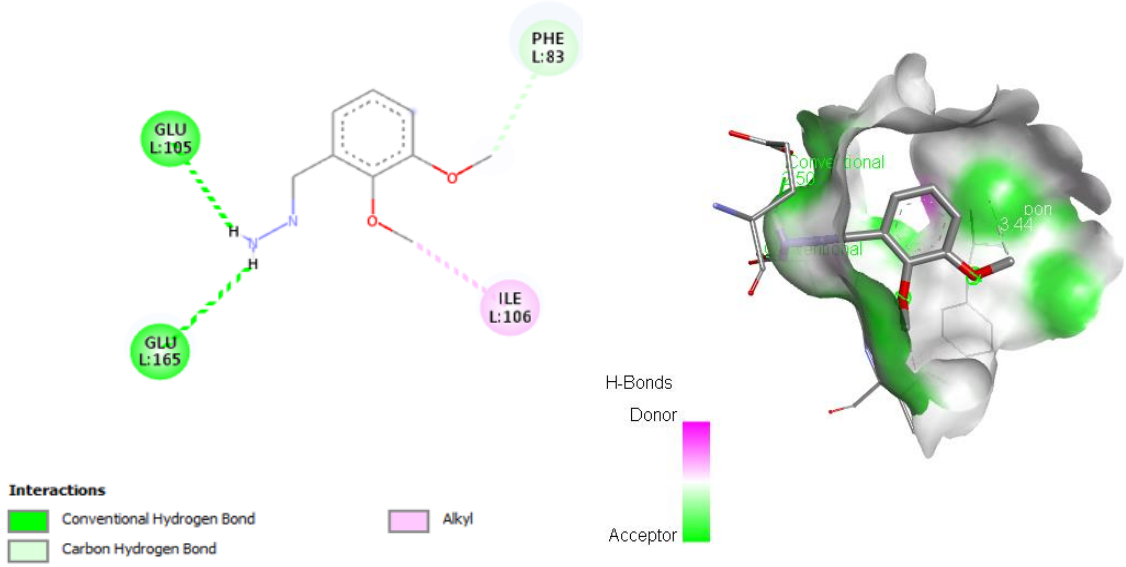

Figure 8. Docking images of compound (E)-1-(2,3-dimethoxybenzylidene) hydrazine (2,3-DMBH) against 7E9B.

Molecular Docking Analysis of 5F90 (Anti-breast Cancer Protein)

Crystal structure of a crenomytilus grayanus lectin in complex with Gb3 allyl, namely 5f90 protein was docked with 2,3-DMBH. In this, the compound exhibited very good binding energy (–4.71 kcal/mol) because of the strong interactions pi-stacked, conventional hydrogen bonding in the angle of 2.29 Å and pi-anion distance in 5.40 Å (shown in Figure 9).

DFT Studies

Figure 10 illustrates the 2,3-DMBH optimized structure obtained by the basis set B3LYP/6-311++ (d,p) with numbering of atoms [40].

Frontier Molecular Orbital Approach

The frontier orbital concepts suggest that the crystal possesses chemical stability. The highest occupied molecular orbital (HOMO) functions as an accepting and donating electron in the lowest

unoccupied molecular orbital (LUMO). The hues red and green, respectively, represent the positive and negative phases [41]. The HOMO-LUMO energy gap for 2,3-DMBH is 4.504 eV. It displays the existence of high and constant excitation energies. The E_{HOMO} is associated with a molecule's ability to disperse electrons, or ionization energy. The ability of a molecule to attach to an electron is known as E_{LUMO}. The energy level of E_{HOMO}-E_{LUMO} indicates whether a molecule is more likely to absorb or donate electrons. The HOMO-LUMO diagram, which shows a summary of the findings is shown in Figure 11. The fragmented HOMO-LUMO energy gap indicates that 2,3-DMBH is an excellent NLO material.

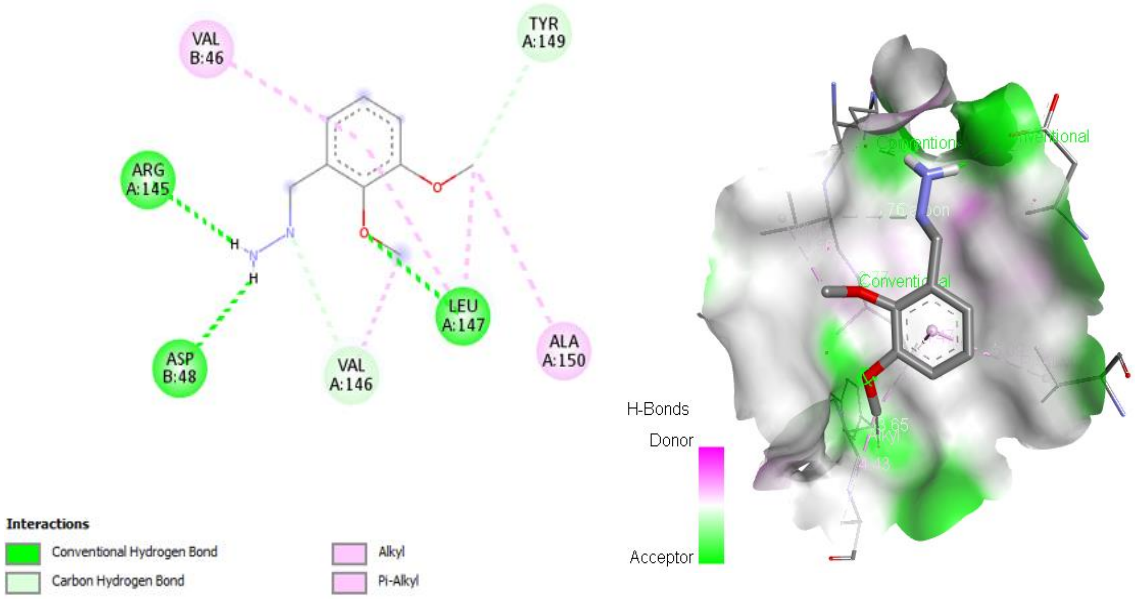

Figure 9. Docking images of compound (E)-1-(2,3-dimethoxybenzylidene) hydrazine (2,3-DMBH) against 5F90.

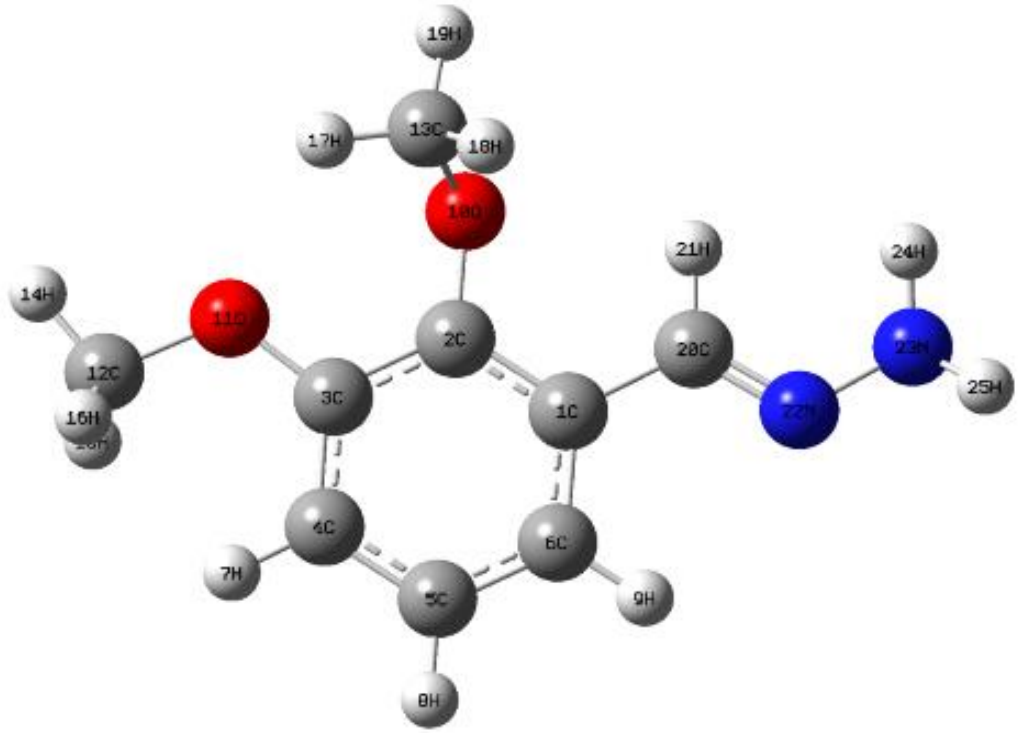

Figure 10. Optimized structure of (E)-1-(2,3-dimethoxybenzylidene) hydrazine (2,3-DMBH).

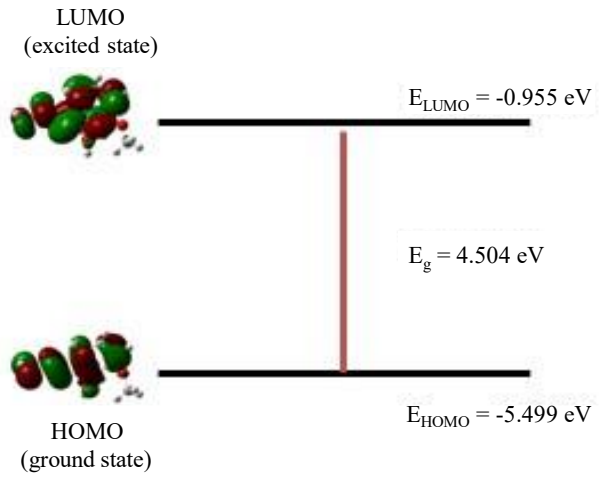

Figure 11. Highest occupied molecular orbital–lowest unoccupied molecular orbital (HOMO-LUMO) diagram of (E)-1-(2,3-dimethoxybenzylidene) hydrazine (2,3-DMBH).

Molecular Electrostatic Potential

A 3D molecular electrostatic potential (MEP) plot for 2,3-DMBH is displayed in Figure 12. Investigating nucleophile and electrophile reactivity is beneficial. The electrophile activity of 2,3-DMBH is shown by the negative area (red color), while the nucleophile activity is represented by the positive part (blue color) [42]. Various hues in the sequence of red, orange, yellow, green, and blue, ranging from (deepest red) to (deepest blue), represent the MEP at the molecule's surface. The color blue represents the strongest attraction, whereas the color red represents the most repulsion. For electrophilic assaults on atoms O and N, which are shown by the color red in Figure 12, the majority of electronegative atoms are located.

Mulliken Atomic Charge of 2,3-DMBH

Figures 13 and 14 display the Mulliken atomic charge distribution for 2,3-DMBH that has been gathered via B3LYP/6-311++ (d,p). Massive, negatively charged atoms are contributors of electrons, whereas positively charged atoms are receivers of electrons. N or O-H atoms may result in the generation of an intermolecular hydrogen connection [39].

Nonlinear Optical Properties

Because of its strong laser harmonic activity, quick NLO response, low insulation constants, rapid electron cloud movement from donor to acceptor, and high NLO susceptibilities, we target this kind of molecule [37, 43–46].

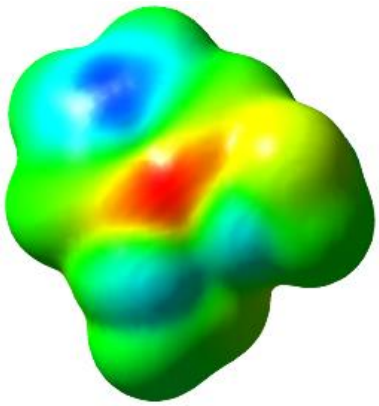

Figure 12. Molecular electrostatic potential (MEP) diagram of (E)-1-(2,3-dimethoxybenzylidene) hydrazine (2,3-DMBH).

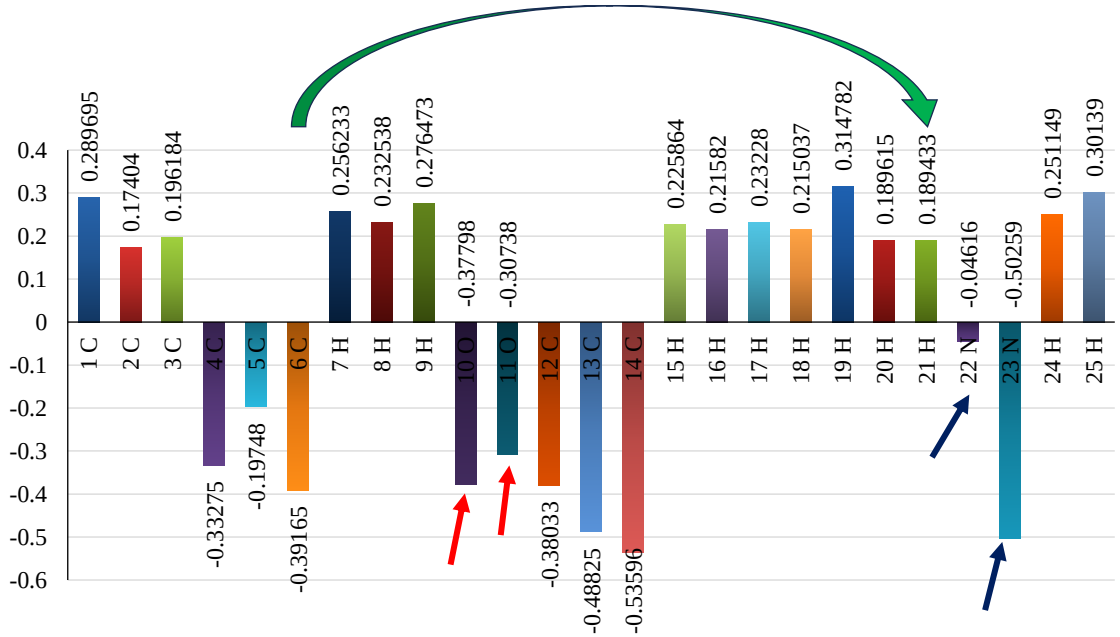

Figure 13. Mulliken atomic charge distribution diagram of (E)-1-(2,3-dimethoxybenzylidene) hydrazine (2,3-DMBH).

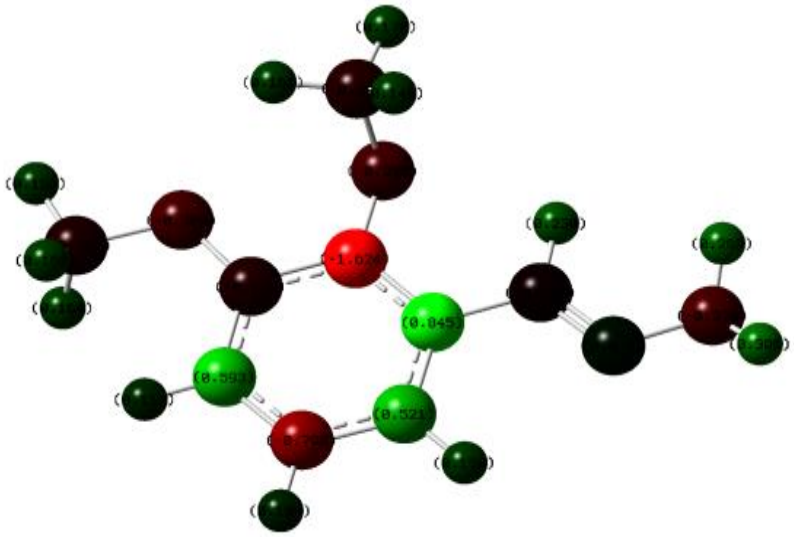

Figure 14. Mulliken atomic charge distribution diagram of (E)-1-(2,3-dimethoxybenzylidene) hydrazine (2,3-DMBH).

Table 6 computes the compound electronic dipole moment, molecular polarizability, and first-order hyperpolarizability of 2,3-DMBH using the B3LYP/6-311++G (d,p) basis set. 3.9336 Debye, 7.4×10^{-23}, and 6.45×10^{-30} esu are the computed values for the total molecule dipole moment, polarizability, and initial hyperpolarizability, respectively. The initial hyperpolarizability parameter of urea has been found to be 0.13×10^{-24} esu. The results indicated that the 2,3-DMBH molecule has an initial hyperpolarizability parameter that is about two times larger than urea's. The ring of aromatics and the accepting and donating functional substituents, C2-H2O2, may both be helpful in explaining the high value of the parameter. The length of the bridge connecting the end groups of the molecules provides an additional reason for the high value of the initial hyperpolarizability. A longer bridge between the donor and acceptor groups may enhance the 2,3-DMBH molecule's nonlinear optical characteristics. This explanation demonstrates that 2,3-DMBH, an organic substance, is a prime example of an NLO active crystal.

Table 6. The molecular electric dipole moment μ (Debye), polarizability (α_0), and first-order hyperpolarizability (β_0) of (E)-1-(2,3-dimethoxybenzylidene) hydrazine (2,3-DMBH).

Dipole Moment	Debye	Hyperpolarizability(β_0)	$\times 10^{-30}$ esu
μ_X	6.4757	β_{XXX}	76.7203
μ_Y	3.4380	β_{YYY}	-4.3049
μ_Z	4.4539	β_{ZZZ}	-1.2632
μ_{TOTAL}	8.5786	β_{XYY}	-2.6337
Polarizability (α_0)	$\times 10^{-23}$ esu	β_{XXY}	-15.043
α_{XX}	-74.93	β_{XXZ}	-33.336
α_{YY}	-67.43	β_{XZZ}	0.9196
α_{ZZ}	-80.74	β_{YZZ}	-9.328
α_{XY}	-4.95	β_{YYZ}	3.2802
α_{XZ}	-11.31	β_{XYZ}	5.7491
α_{YZ}	0-0.29	β_0	6.45393
α_0	7.4×10^{-23}		

SUMMARY

Using conventional technique, (E)-1-(2,3-dimethoxybenzylidene) hydrazine (2,3-DMBH) was synthesized at ambient temperature. The synthesized product was characterized by the spectral techniques like FT-IR, ^{1}H-NMR, ^{13}C-NMR. The stretching vibrational frequencies at 1621.50 cm^{-1} confirms the presence of HC=N bond. In the ^{1}H-NMR spectrum, the singlet at 8.999 ppm confirms the HC=N proton, and it correlates the 12 protons of 2,3-DMBH compound. In the ^{13}C-NMR spectrum of 2,3-DMBH has 9 signals and it correlates the 9 carbons of the 2,3-DMBH compound. UV-visible spectrum shows the maximum absorbance at 390 nm. The value of energy band gap at 4.69 eV and lower cut-off wavelength shows that the grown title material is suitable for the photonics and optical applications. The effectiveness of the produced compounds as drug candidates was also assessed using ADME calculations and Lipinski's rule verification. The molecular docking studies of the synthesized compounds 3(a-g) against six different proteins (3ERT, 3EWD, 7E9B, and 5F90) were carried out using AUTO DOCK software and obtained very good promising results. The compound 2,3-DMBH has good binding value against all the proteins in the order of 3ERT > 5F90 > 7E9B > 3EWD protein with respective binding energy in kcal/mol of -5.44 > -4.71 > -4.49 > -4.43. From the discussion 2,3-DMBH has act as a good drug candidate. DFT quantum mechanical studies were used to explain stability, ICT reactions. From the frontier molecular orbital theory, bandgap between HOMO and LUMO is calculated and it is 3.25 eV. MEP describes the mapping of nucleophilic and electrophilic activity of 2,3-DMBH by color codes deepest red to deepest blue. Mulliken charge of electronegativity illustrates ICT reaction between N—H and O—H. The first-order hyperpolarizability value of 2,3-DMBH was calculated using quantum mechanical calculations of DFT program in the basis set of B3LYP/6-311++ (d, p). The first-order hyperpolarizability value of 2,3-DMBH is greater than that of urea value. From this evidence 2,3-DMBH is a good NLO active crystal and it may be applied to optical and laser safety gadgets.

CONCLUSION

The synthesized Schiff base, (E)-1-(2,3-dimethoxybenzylidene)hydrazine (2,3-DMBH), was confirmed through spectral and computational studies. It exhibited strong chemical stability, notable NLO properties, and a suitable energy band gap for optical applications. ADMET analysis and molecular docking revealed its potential as a drug candidate with good bioavailability and binding affinity. Overall, 2,3-DMBH shows promise for applications in both photonic and pharmaceutical fields.

REFERENCES

1. Punitha P, Senthilkumar S, Muthukumaran G. Synthesis and characterization of (E)-4-amino-N'-(2,5-dimethoxybenzylidene) benzohydrazide. Chem Data Collect. 2020; 28: 100373. doi: 10.1016/j.cdc.2020.100373.

2. Enbaraj E, Jeyashri KR, Logeshwari G, Manikandan H, Sivakumar K. Synthesis, crystal structure, Hirshfeld surface analysis and theoretical studies of bis-substituted benzylidene ethan-1,2-diamines. J Mol Struct. 2023; 1275: 134605. doi: 10.1016/j.molstruc.2022.134605.
3. Guerroudj AR, Boukabcha N, Benmohammed A, Dege N, Belkafouf NEH, Khelloul N, et al. Synthesis, crystal structure, vibrational spectral investigation, intermolecular interactions, chemical reactivity, NLO properties and molecular docking analysis on E-N-4-nitrobenzylidene-3-chlorobenzenamine—a combined experimental and theoretical study. J Mol Struct. 2021; 1240: 130589. doi: 10.1016/j.molstruc.2021.130589.
4. Meenatchi V, Agilandeshwari R, Meenakshisundaram SP. Synthesis, structure, characterization and theoretical studies of NLO active furan-2-carbohydrazide monohydrate derivative single crystals. RSC Adv. 2015; 5 (87): 71076–71087. doi: 10.1039/C5RA07936E.
5. Dhanalakshmi M, Parthiban S. Synthesis, structure, supramolecular architecture and Hirshfeld surface analysis of 4-aminobenzene-1-sulfonic acid with 18-crown-6. Chem Data Collect. 2020; 28: 100472. doi: 10.1016/j.cdc.2020.100472.
6. Rajesh NP, Jabha Ananthi V, Vinitha G. Investigations on single crystal growth and nonlinear optical studies of 2-hydroxy-1-naphthaldehyde. J Cryst Growth. 2019; 511: 25–32. doi: 10.1016/j.jcrysgro.2019.01.017.
7. Kamaal S, Mehkoom M, Ali A, Afzal SM, Alam MJ, Ahmad S, et al. Potential third-order nonlinear optical response facilitated by intramolecular charge transfer in a simple Schiff base molecule—experimental and theoretical exploration. ACS Omega. 2021; 6 (9): 6185–6194. doi: 10.1021/acsomega.0c05557.
8. Sarma S, Bhowmik A, Sarma MJ, Banu S, Phukan P, Das DK. Condensation product of 2-hydroxy-1-napthaldehyde and 2-aminophenol: selective fluorescent sensor for Al^{3+} ion and fabrication of paper strip sensor for Al^{3+} ion. Inorg Chim Acta. 2018; 469: 202–208. doi: 10.1016/j.ica.2017.09.025.
9. Rao PV, Rao CP, Wegelius EK, Rissanen K. 2-Hydroxy-1-naphthaldehyde-derived Schiff bases: synthesis, characterization, and structure. J Chem Crystallogr. 2003; 33: 139–147. doi: 10.1023/A:1023226925997.
10. Taki AG, Rahman AA, Azzouz ASP. The influence of pH and temperature on tautomerism of imines derived from 2-hydroxy-1-napthaldehyde. Iraqi Natl J Chem. 2005; 20: 568–585.
11. Zhou D, Sun C, Chen C, Cui X, Li W. Research of a highly selective fluorescent chemosensor for aluminum (III) ions based on photoinduced electron transfer. J Mol Struct. 2015; 1079: 315–320. doi: 10.1016/j.molstruc.2014.09.050.
12. Murukan B, Mohanan KK. Synthesis, characterization, electrochemical properties and antibacterial activity of some transition metal complexes with [(2-hydroxy-1-naphthaldehyde)-3-isatin]-bishydrazone. Transit Met Chem. 2006; 31 (4): 441–446. doi: 10.1007/s11243-006-0011-7.
13. Özbek N, Kavak G, Özcan Y, Ide S, Karacan N. Structure, antibacterial activity and theoretical study of 2-hydroxy-1-naphthaldehyde-*N*-methylethanesulfonylhydrazone. J Mol Struct. 2009; 919 (1–3): 154–159. doi: 10.1016/j.molstruc.2008.09.010.
14. Chohan ZH, Shad HA. Structural elucidation and biological significance of 2-hydroxy-1-naphthaldehyde derived sulfonamides and their first-row d-transition metal chelates. J Enzyme Inhib Med Chem. 2008; 23 (3): 369–379. doi: 10.1080/14756360701585692.
15. Agbom-Uzim MU, Sani U. Synthesis, characterization, cytotoxicity and antimicrobial activities of Co(II) and Ni(II) complexes of Schiff base derived from 2-hydroxy-1-naphthaldehyde and ethylamine. Appl J Environ Eng Sci. 2022; 8 (3): 200–214. doi: 10.48422/IMIST.PRSM/ajees-v8i3.33232.
16. Kimura R, Yabuuchi T, Hisaki M, Sugimoto H, Ohyama A, Mochida K. Studies on the synthesis of new antimicrobials. I. Synthesis of 2,5-dichloroaniline derivatives and their some antibacterial activities. Chem Pharm Bull. 1962; 10 (12): 1226–1232. doi: 10.1248/cpb.10.1226.
17. Lovejoy DB, Richardson DR, Bernhardt PV. 2-Hydroxy-1-naphthaldehyde 2-methylthiosemicarbazone. Acta Crystallogr C Cryst Struct Commun. 2000; 56 (3): 341–342. doi: 10.1107/S0108270199015140.

18. Dziembowska T, Rozwadowski Z, Filarowski A, Hansen PE. NMR study of proton transfer equilibrium in Schiff bases derived from 2-hydroxy-1-naphthaldehyde and 1-hydroxy-2-acetonaphthone. Deuterium isotope effects on ^{13}C and ^{15}N chemical shifts. Magn Reson Chem. 2001; 39 (S1): S67–S80. doi: 10.1002/mrc.949.
19. Asiri AM, Badahdah KO. Synthesis of some new anils part 1: reaction of 2-hydroxy-benzaldehyde and 2-hydroxynaphthaldehyde with 2-aminopyridene and 2-aminopyrazine. Molecules. 2007; 12 (8): 1796–1804. doi: 10.3390/12081796.
20. Sadia M, Naz R, Khan J, Khan R. Synthesis and evaluation of a Schiff-based fluorescent chemosensor for the selective and sensitive detection of Cu^{2+} in aqueous media with fluorescence off-on responses. J Fluoresc. 2018; 28: 1281–1294. doi: 10.1007/s10895-018-2278-4.
21. Ünver H. Synthesis and spectroscopic studies in some new Schiff bases. Spectrosc Lett. 2001; 34 (6): 783–791. doi: 10.1081/SL-100107900.
22. Das AK, Goswami S. 2-Hydroxy-1-naphthaldehyde: a versatile building block for the development of sensors in supramolecular chemistry and molecular recognition. Sens Actuators B Chem. 2017; 245: 1062–1125. doi: 10.1016/j.snb.2017.01.068.
23. Antonov L, Fabian WM, Nedeltcheva D, Kamounah FS. Tautomerism of 2-hydroxynaphthaldehyde Schiff bases. J Chem Soc Perkin Trans. 2000; 2 (6): 1173–1179. doi: 10.1039/B000798F.
24. Yıldız M, Ünver H, Erdener D, Ocak N, Erdönmez AN, Durlu TN. Tautomeric properties and crystal structure of *N*-[2-hydroxy-1-naphthylidene] 2,5-dichloroaniline. Cryst Res Technol. 2006; 41 (6): 600–606. doi: 10.1002/crat.200510632.
25. Rajaram V, Paulraj K, Ramalingam SK. Dioxouranium (VI) complexes of some bidentate Schiff bases. Transit Met Chem. 1983; 8: 335–337. doi: 10.1007/BF00618565.
26. Sekar J, Ganesan M, Manivel K, Srinivasan P. Physiochemical properties optimization of synthetic bio-destructible 2,6-bisarylidene-4-(*t*-butyl) cyclohexanones to select a potential anti-cancer drug contender. J Mol Struct. 2025; 1324: 140836. doi: 10.1016/j.molstruc.2024.140836.
27. Wathoni N, Shan CY, Shan WY, Rostinawati T, Indradi RB, Pratiwi R, Muchtaridi M. Characterization and antioxidant activity of pectin from Indonesian mangosteen (*Garcinia mangostana* L.) rind. Heliyon. 2019; 5 (8): e02299. doi: 10.1016/j.heliyon.2019.e02299.
28. Meenambigai G, Sekar J, Kandasamy SP, Srinivasan P. Design, synthesis, spectral characterization, in silico ADMET studies, molecular docking, antimicrobial activity, and anti-breast cancer activity of 5,6-dihydrobenzo[H]quinazolines. J Mol Struct. 2024; 1296: 136771. doi: 10.1016/j.molstruc.2023.136771.
29. Rakini A, Rajarajan K, Neela M. Growth, characterization and second harmonic generation NLO activity of semi-organic crystal: L-arginine picrate crystal doped with nickel chloride. J Mater Sci Mater Electron. 2024; 35: 706. doi: 10.1007/s10854-024-12445-3.
30. Maheswari R, Rajarajan K, Rakini A, et al. Crystal growth and characterization of L-tryptophan doped zinc bis thiourea sulphate (TDZBTS) crystal using UV-visible, FT-IR spectral studies, thermal studies, P-XRD & SEM-EDAX. Mater Today Proc. 2023. In press. doi: 10.1016/j.matpr.2023.04.325.
31. Yogeswari C, Girisun TS, Nagalakshmi R. Electrospun 2-nitroaniline (2NA)–poly (methylmethacrylate) (PMMA) nanofibers for power limiting and Q-switching applications. Chem Phys Lett. 2022; 786: 139209. doi: 10.1016/j.cplett.2021.139209.
32. Dhanalakshmi M, Balakrishnan C, Ahamed SR, Vinitha G, Parthiban S. Synthesis, structural characterization, Hirshfeld surface analysis and third-order nonlinear optical properties of Schiff bases derived from 1,1-diphenylmethylamine. J Mol Struct. 2022; 1251: 131942. doi: 10.1016/j.molstruc.2021.131942.
33. Steffy AD, Dhas DA, Joe IH, Gunasekaran B, Vinitha G. Experimental and theoretical investigation on piperazine-1,4-diium bis(2,5-dichlorophenoxyacetate) single crystal: a potential candidate for nonlinear optical applications. J Mol Struct. 2023; 1285: 135520. doi: 10.1016/j.molstruc. 2023.135520.
34. Subramaniyan R, Ramarajan R, Ramalingam A, Sambandam S, Petersamy A, Guerroudj AR, et al. Microwave-assisted synthesis, vibrational spectra, Hirshfeld surface and interaction energy, DFT, topology, in silico ADMET and molecular docking studies of 1,2-bis(4-methoxybenzylidene) hydrazine. J Mol Struct. 2023; 1278: 134946. doi: 10.1016/j.molstruc.2023.134946.

35. Ramkumar S, Rajalakshmi R. Synthesis, spectral, single crystal XRD structure, Hirshfeld surface, molecular docking and in silico ADMET studies of symmetrical azine: 1,2-bis(4-(methylthio)benzylidene)hydrazine. Mater Today Proc. 2023. In press. doi: 10.1016/j.matpr.2023.05.63.
36. Meenambigai G, Sekar J, Rajendran AS, Srinivasan P. A splendid comprehension into in-silico and in-vitro biological investigations to assess the anti-inflammatory and anti-breast cancer activities of newly synthesized 1-phenylethyl quinoline-4-carboxylates. J Mol Struct. 2024; 1311: 138411. doi: 10.1016/j.molstruc.2024.138411.
37. Reena P, Joema SE, Gunasekaran B, et al. Scrutinizing the optical limiting action of a novel carbonyl guanidinium hippurate for laser safety device applications. Opt Mater. 2022; 132: 112749. doi: 10.1016/j.optmat.2022.112749.
38. Borisenko VE, Grishanova ON. Hydrogen bond and electro-optical parameters of chlorosubstituted aniline. J Mol Struct. 1990; 239: 13–21. doi: 10.1016/0022-2860(90)80198-S.
39. Kang Y, Zheng XJ, Jin LP. A microscale multi-functional metal-organic framework as a fluorescence chemosensor for Fe(III), Al(III) and 2-hydroxy-1-naphthaldehyde. J Colloid Interface Sci. 2016; 471: 1–6. doi: 10.1016/j.jcis.2016.03.008.
40. Ramkumar S, Ramarajan R. Green synthesis, single-crystal X-RD, Hirshfeld analysis and anti-Covid-19 molecular docking investigation of symmetrical azines. ChemistrySelect. 2023; 8 (6): e202204494. doi: 10.1002/slct.202204494.
41. Boukabcha N, Djafri A, Megrouss Y, et al. Synthesis, crystal structure, spectroscopic characterization and nonlinear optical properties of Z-N'-(2,4-dinitrobenzylidene)-2-(quinolin-8-yloxy) acetohydrazide. J Mol Struct. 2019; 1194: 112–123. doi: 10.1016/j.molstruc.2019.05.074.
42. Kansız S, Dege N. Synthesis, crystallographic structure, DFT calculations and Hirshfeld surface analysis of a fumarate bridged Co(II) coordination polymer. J Mol Struct. 2018; 1173: 42–51. doi: 10.1016/j.molstruc.2018.06.071.
43. Serli BFY, Adliani N. Synthesis, characterization and computational studies of novel (E)-N-(3,4-dimethoxybenzylidene) naphthalen-1-amine. J Sci Appl Technol. 2019; 2 (1): 35–39. doi: 10.35472/281457.
44. Kansiz S, Dege N, Ozturk S, et al. Crystal structure and Hirshfeld surface analysis of 2-methyl-3-nitro-N-[(E)-(5-nitrothiophen-2-yl) methylidene] aniline. Acta Crystallogr Sect E Crystallogr Commun. 2021; 77 (2): 138–141. doi: 10.1107/S2056989021000529.
45. Simsek O, Ashfaq M, Tahir MN, Ozturk S, Agar E. Synthesis and characterizations of the Schiff base derived from 2-hydroxy-5-nitrobenzaldehyde along with Hirshfeld surface analysis and computational study. J Struct Chem. 2023; 64 (5): 942–953. doi: 10.1134/S0022476623050128.
46. Priyadarshani N, Girisun TS, Rao SV. Improved femtosecond third-order nonlinear optical properties of thin layered Cu_3Nb_2O. Opt Mater. 2019; 88: 586–593. doi: 10.1016/j.optmat.2018.12.034.
47. Rakini A, Rajarajan K, Ruban R, Maheswari R, Malathy S, Swetha G, et al. Synthesis and characterization studies of glycine 4-nitrophenolate crystal doped with nickel chloride. Mater Today Proc. 2023. In press. doi: 10.1016/j.matpr.2023.02.114.

